Supporting Information

Chan et al. 10.1073/pnas.1423009112

SI Materials and Methods

Single-Cell Analysis. Cell cycle status was determined using Vybrant DyeCycle (Life Technologies) according to the manufacturer's protocol. Fluorescence microscopy images were captured using the DAPI filter channel. The intensity in the cell with two nuclei served as a reference for the G_2/M phase of the cell cycle. A cell in the G_1 phase was characterized as having one-half of the reference fluorescence intensity. Any cell with a fluorescence intensity falling between the G_1 and G_2/M phases was classified as being in S phase. Purinosome density was defined as the number of purinosomes per cell, and purinosome size was defined as the average size within a single cell.

Data acquisition setup. Unless specified otherwise, all of the images analyzed in this study were obtained with a Nikon Apo TIRF 100× oil objective lens (NA 1.49) at a scale of 0.072 μm/pixel. In each cell, FGAMS-GFP and Vybrant DyeCycle channels were captured sequentially. For FGAMS-GFP, the filter cube was custom-designed by Chroma Technology, with an exposure time of 2 s. For Vybrant DyeCycle, staining was done using standard filter cube 49000-ET-DAPI, with an exposure time of 10 ms.

Image capture and data analysis in a single cell. To determine the purinosome content and cell cycle phase of each single cell, we captured images from both FGAMS-GFP and Vybrant DyeCycle staining (Fig. S1 *A*–*C*). First, the image showing Vybrant DyeCycle staining was converted to an 8-bit format (Image → Type → 8-bit) in ImageJ. Then the fluorescent intensity of the nucleus was measured and background-subtracted (Fig. S1*D*). Finally, purinosome size and number were analyzed using the "Analyze Particle" function of ImageJ.

Each image from FGAMS-GFP channel was converted to 8-bit format (Fig. S2*A*). The contrast was inverted (Image → Lookup Tables → Invert LUT) (Fig. S2*B*), and the background was subtracted (Process → Subtract Background → Rolling ball radius, between 5 and 10 pixels) (Fig. S2*C*), so that the appearance of the purinosomes most closely resembled the original FGAMS-GFP image (Fig. S2*A*). After the background was subtracted, image threshold was set before analysis (Image → Adjust → Threshold → Set) (Fig. S2*D*). Finally, the scale of the image was set at 0.072 μm/pixel (Analyze → Set Scale), and purinosome size (area) and number were analyzed [Analyze → Analyze Particles → Size (0-Infinity); Circularity (0.00–1.00)] (Fig. S2*E*). Purinosome size was converted from area to diameter.

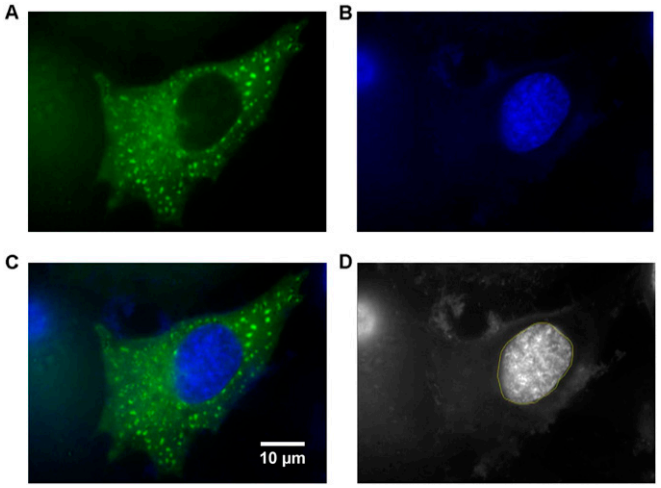

Fig. S1. Cell cycle image analysis of purinosome-positive cells. (*A*) Fluorescence image of a purinosome-positive HeLa cell transiently transfected with FGAMS-GFP under purine-depleted growth conditions. (*B*) Vybrant DyeCycle staining of the same cell to determine cell cycle status. (*C*) Merged image of *A* and *B*. (*D*) Gated area selected for fluorescence intensity measurements (yellow outline).

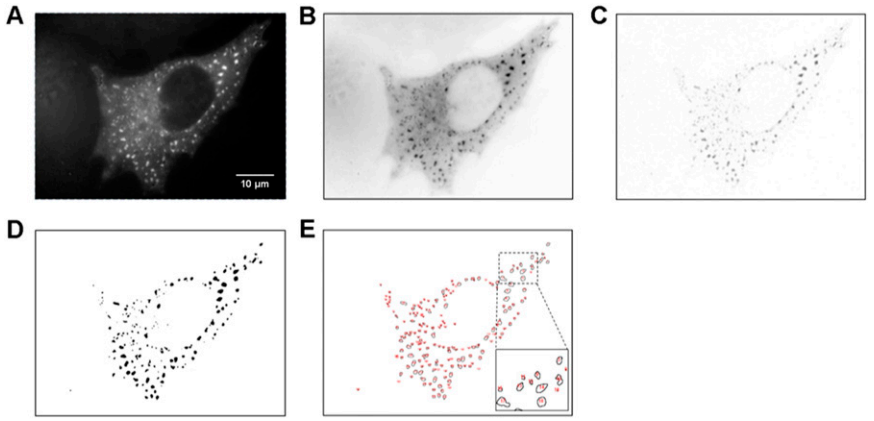

Fig. S2. Image analysis of purinosome size and number. (*A*) Original FGAMS-GFP image in 8-bit format. (*B*) Image contrast inverted. (*C*) Background-subtracted image. (*D*) Threshold of the image set. (*E*) Results of the particle analysis.

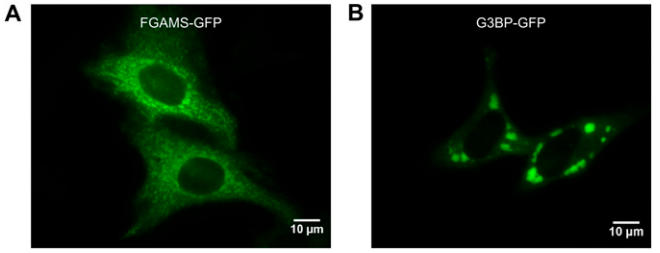

Fig. S3. Comparison of the images of HeLa cells transfected with FGAMS-GFP and G3BP-GFP. (*A*) Representative fluorescence images of cells showing purinosome formation under cell synchronization at G_1 phase. (*B*) Representative fluorescence image of cells showing stress granules under DB-cAMP treatment.

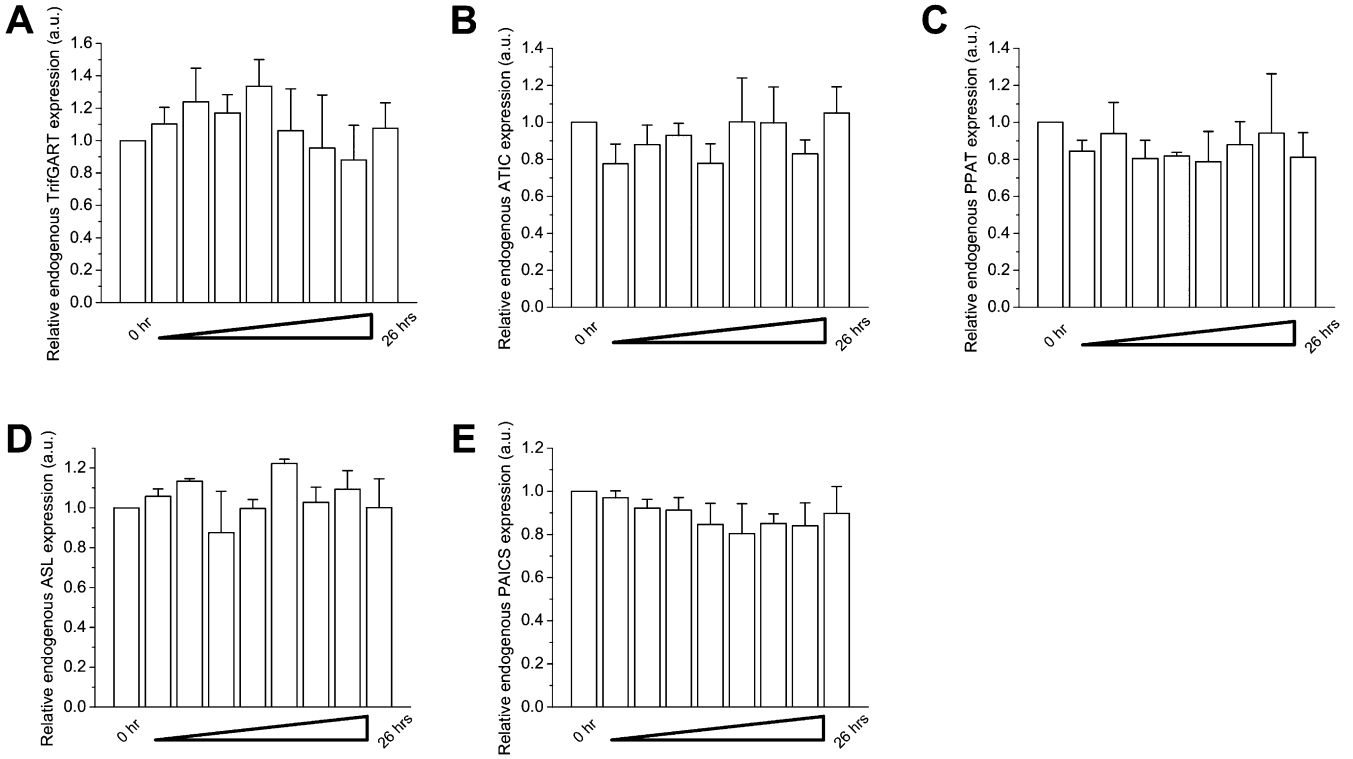

Fig. S4. Statistical analyses of endogenous (*A*) TrifGART, (*B*) ATIC, (*C*) PPAT, (*D*) ASL, and (*E*) PAICS as a function of time posttransfection of FGAMS-GFP.

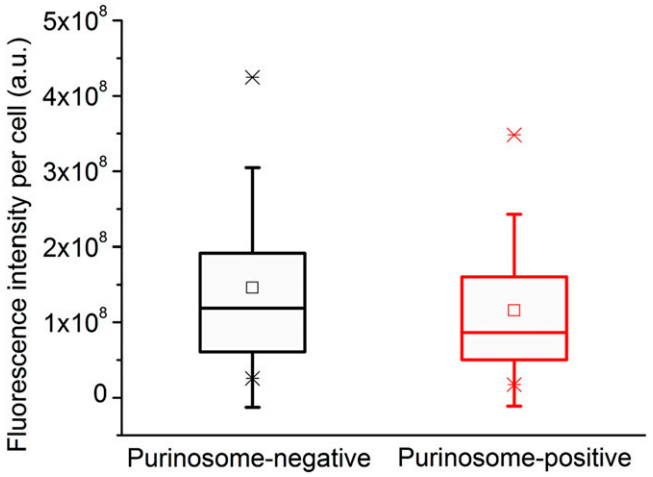

Fig. S5. Fluorescence intensity per cell for both purinosome-negative and -positive HeLa cells (n = 50).

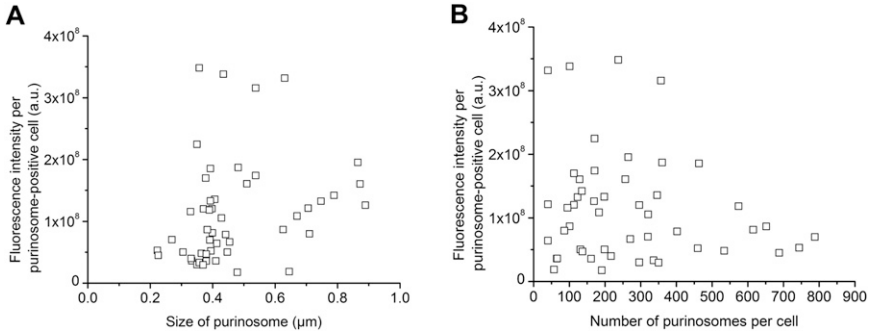

Fig. S6. Fluorescence intensity per purinosome-positive HeLa cell as a function of average purinosome size (*A*) and number of purinosomes per cell (*B*). The results indicate no correlation between fluorescence intensity per cell with either average purinosome size or number of purinosomes per cell.

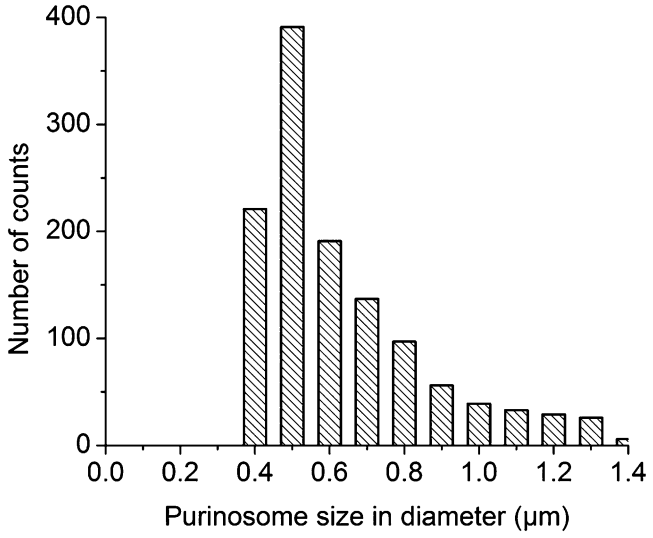

Fig. S7. Size distribution of purinosomes measured by STORM. Shown is the number of counts with respect to purinosome size in HeLa cells transfected with FGAMS-mEos2. These results are highly consistent with the range of purinosome size shown in Fig. 3.

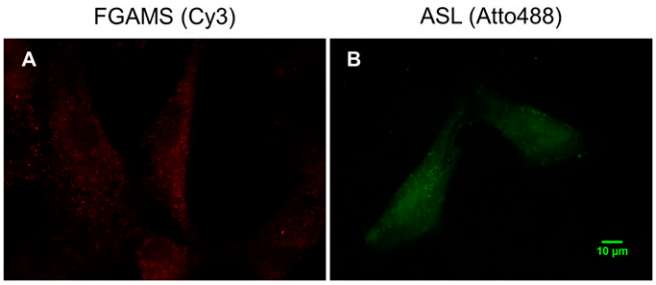

Fig. S8. Immunofluorescence imaging of FGAMS and ASL in fixed LND fibroblast cells. HGPRT-deficient LND fibroblast cells were cultured in DMEM growth medium supplemented with 2 mM glutamine, fixed with 4% (vol/vol) formaldehyde, and permeabilized with 0.2% Triton X-100 before being stained with (*A*) Cy3-labeled FGAMS and (*B*) Atto488-labeled ASL antibodies.

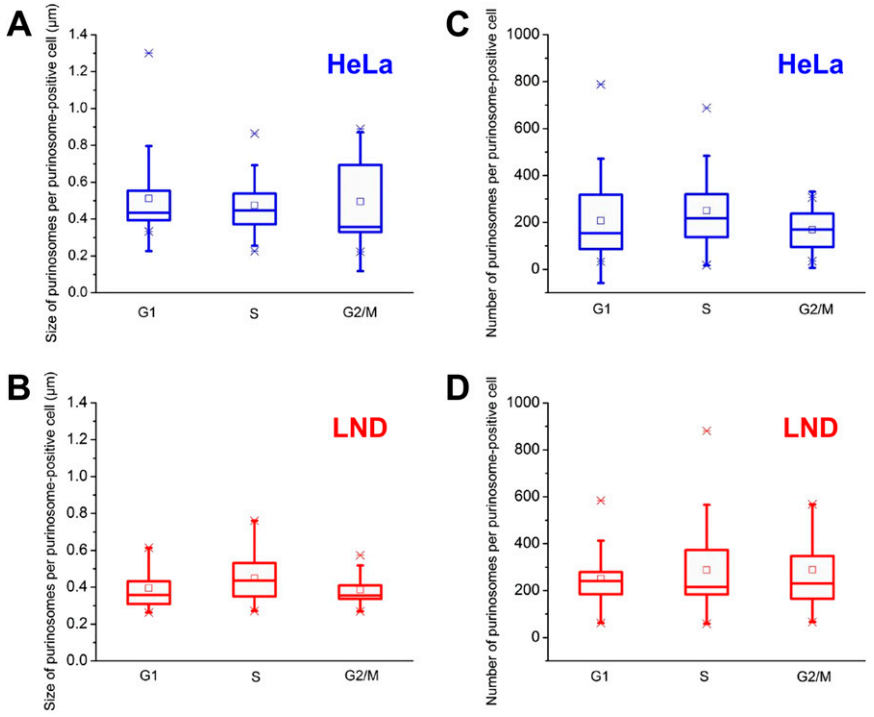

Fig. S9. Distribution of average size and number of purinosomes in a purinosome-positive cell as a function of cell cycle phase. Shown are boxplots of the average purinosome size as a function of cell cycle phase in HeLa (*A*) and LND (*B*) fibroblast cells and of the number of purinosomes in purinosome-positive HeLa (*C*) and LND (*D*) fibroblast cell in a given phase of the cell cycle. One-way ANOVA was carried out in individual plots, and all *P* values were >0.1, suggesting that the differences are not significant (*A*, $P = 0.662$; *B*, $P = 0.128$; *C*, $P = 0.398$; *D*, $P = 0.642$).